

A technique for processing lidar measurements of backscattering matrices

S.N. Volkov, B.V. Kaul', and I.V. Samokhvalov¹

Institute of Atmospheric Optics, Siberian Branch of the Russian Academy of Sciences, Tomsk
¹*Tomsk State University*

Received March 22, 2002

A technique is developed for calibration of a lidar used to measure backscattering matrices (BSM). The technique exploits the fact that the well-known molecular backscattering matrix $\sigma = \Sigma/\Sigma_{11}$ normalized to the element Σ_{11} is independent of the air density. An algorithm is described for separation of the aerosol component from BSM of an aerosol-gas mixture and estimation of errors in determination of BSM elements from a single measurement. The latter gives a criterion of quality of the obtained results to be used in the further BSM analysis.

Introduction

Particles of upper-layer clouds have a crystal nature, are significantly anisometric and, consequently, can occupy some dominant positions in space. This circumstance leads to a considerable anisotropy in light scattering that should be taken into account in the problems connected with light propagation through the atmosphere. The information about the shape and orientation of particles can be obtained from scattering matrices, therefore light backscattering matrices (BSM) are a matter of our scientific enquiry over a period of years.

The instrumentation is described in Refs. 1–3. The signal preprocessing methods, namely, allowance for counting losses, as well as aftereffect noise and mean noise due to background illumination, are kept unchanged. These methods were then complemented with statistical smoothing of a signal.⁴ At the same time, the method of calibration and the algorithm for calculation of BSM elements have been changed significantly as compared to the simplified version used at the initial stage, and they remain unpublished yet. The aim of this paper is to fill this gap. This publication is also needed, because in the nearest future we plan to publish the results of statistical analysis of BSM data. Simplifications at the initial stage of the study concerned the following points.

First, the bases, in which the Stokes vectors of the laser radiation and the scattered radiation coming to the source are determined, were assumed exactly matched. In other words, the direction of the axis x of the source's basis coincides with the direction of the axis x of the receiver's basis. However, because of errors in mutual positioning of polarization elements of the source and receiver, the matching may be inexact. This will affect the components of the receiver's instrumental vectors, which in their turn, are assumed known exactly. The latter supposes, in particular, exact knowledge of phase shifts introduced by the phase plate. However, the

manufacturer gives the error of about 1.5–2° in this parameter. Besides, as was shown by specialized studies, the available plates are subject to thermal drift within several degrees because of insufficient temperature compensation.

One more source of errors may be the drift of quantum efficiencies of counting channels. For calculations, it is important to know the ratio of efficiencies of the channels measuring the power of two light fluxes formed as a result of passage of the scattered radiation through the Wollaston prism. The ratio is determined by the calibration against a source of unpolarized radiation before the beginning of measurements.³ However, the PMT sensitivity may change during measurements due to rather powerful illumination from the lidar's near zone, and this change can hardly be controlled. To decrease the effect of the above factors, we have developed a technique for lidar calibration against the "molecular reference."

Second, at the initial stage we ignored the redistribution of contributions from the molecular and aerosol scatterings inside a cloud. Therefore, the found BSM can be rigorously referred to cloud particles only in the case of large ($R > 10$) scattering ratios. The latter is determined as the ratio of the sum of the molecular and aerosol backscattering coefficients to the molecular backscattering coefficient:

$$R(h) = [\beta_a(h) + \beta_m(h)]/\beta_m(h). \quad (1)$$

This simplification was then removed, but our more rigorous approach was not published by us and is considered below.

1. Lidar calibration against "molecular reference"

The process of BSM measurement is reduced to measurement of 12 pairs of discrete series of numbers of photoelectronic pulses $N(h_n)$ coming in the n th time strobe of the photon counter. From here on, the index n

emphasizing the discrete character of signals will be omitted in equations for simplicity. The values of $N(h)$ are determined by the lidar equations written in the single-scattering approximation³:

$$\begin{aligned} N_k^{(1)}(h) &= \kappa_1 \Delta h N_0 A h^{-2} T^2(h) \mathbf{G}_j \mathbf{M}(h) \mathbf{S}_i, \\ N_k^{(2)}(h) &= \kappa_2 \Delta h N_0 A h^{-2} T^2(h) \mathbf{G}_j^* \mathbf{M}(h) \mathbf{S}_i, \end{aligned} \quad (2)$$

$$k = 3(i-1) + j; \quad i = 1, 2, 3, 4; \quad j = 1, 2, 3,$$

where $N_k^{(1)}(h)$ and $N_k^{(2)}(h)$ are the numbers of the pulses in the first and second channels measuring the mutually normally polarized light fluxes formed after passage of the scattered radiation through the Wollaston prism. The superscript (1) corresponds to the component with the linear polarization along the axis x , and the superscript (2) corresponds to the component polarized along the axis y of the receiver's polarization basis. The subscripts i and j stand, respectively, for the number of the polarization state of the laser radiation and for the number of the pair of the receiver's instrumental vectors, which will be discussed below; κ_1 and κ_2 are quantum efficiencies of the counting channels; h and Δh are the height corresponding to the n th time strobe of the photon counter and the spatial length of the n th strobe; N_0 is the number of photons in the laser pulse; A is the antenna area; $T(h)$ is the transparency of a path section $[0, h]$; \mathbf{G}_j , \mathbf{G}_j^* ($j = 1, 2, 3$) represent three pairs of mutually orthogonal instrumental vectors; $\mathbf{M}(h)$ is the backscattering matrix; \mathbf{S}_i ($i = 1, 2, 3, 4$) is the Stokes vector of the laser radiation normalized to the intensity.

The instrumental row vectors³ have the following components:

$$\mathbf{G}_j = (1, x_j, y_j, z_j); \quad \mathbf{G}_j^* = (1, -x_j, -y_j, -z_j). \quad (3)$$

Their mutual orthogonality is guaranteed by the fact that at all j the last polarization device on the path of the scattered radiation is the Wollaston prism, whose action replaces installation of a linear polarizer in crossed positions.

In the general case, we denote the Stokes vectors of the source laser radiation normalized to the intensity as column vectors:

$$\mathbf{S}_i = (1, q_i, u_i, v_i)^T. \quad (4)$$

In our case, they have fixed values:

$$\begin{aligned} \mathbf{S}_1 &= (1, 1, 0, 0)^T; \quad \mathbf{S}_2 = (1, -1, 0, 0)^T; \\ \mathbf{S}_3 &= (1, 0, 1, 0)^T; \quad \mathbf{S}_4 = (1, 0.11, 0.28, 0.95)^T. \end{aligned}$$

The letter T denotes transposition. The accuracy of the first three vectors is provided for by the use of the Glan prism in the source's polarization attachment. The fourth polarization is somewhat different from the circular one, because the plates used in the laser's polarization attachment are not exactly $\lambda/4$. Therefore, values of the components of \mathbf{S}_4 result from specialized measurements.

Twelve parameters are calculated from the values determined by Eqs. (2)

$$C_k(h) = \frac{N_k^{(1)}(h) - N_k^{(2)}(h)}{N_k^{(1)}(h) + N_k^{(2)}(h)} = \frac{[\mathbf{G}_j \mathbf{M}(h) - \alpha_j \mathbf{G}_j^* \mathbf{M}(h)] \mathbf{S}_i}{[\mathbf{G}_j \mathbf{M}(h) + \alpha_j \mathbf{G}_j^* \mathbf{M}(h)] \mathbf{S}_i} \quad (5)$$

where $\alpha_j = \kappa_{2j}/\kappa_{1j}$ is the ratio of quantum efficiencies of the counting channels. The index j emphasizes the fact that this parameter can be subject to drift during measurements.

Calibration against the molecular scattering is based on the assumption that molecular scattering prevails at some part of the sensing path.⁵ Unlike Ref. 1, which considers the ratio of the aerosol and molecular backscattering coefficients, here we consider the ratios between BSM elements. In this case, the problem of selection of the calibration part is solved more reliably, because one more criterion appears in addition to the ordinary ones. The thing is that, with the ideal lidar parameters presented in Ref. 3, the parameters C_k are, in essence, the Stokes parameters normalized to the intensity. Really, they are shifted estimates, which, nevertheless, are characterized by invariance and relative closeness to the Stokes parameters expected at molecular scattering provided BSM corresponds to molecular scattering. In our case, at the path's sections, where the molecular scattering prevails, we should expect $C_k = \text{const}$; with the absolute values of C_k close to unity at $i = j$ and close to zero at $i \neq j$. This behavior is the consequence of the corresponding selection of \mathbf{S}_i and the diagonal form of the normalized molecular BSM, which is defined as matrix σ with the components

$$\begin{aligned} \sigma_{11} &= 1, \quad \sigma_{22} = \sigma, \quad \sigma_{33} = -\sigma, \quad \sigma_{44} = -\sigma, \\ \sigma_{mm} &= 0, \quad \text{if } m \neq n, \\ \sigma &= 0.97. \end{aligned} \quad (6)$$

At the path's section with this behavior of the profiles $C_k(h)$, we select the calibration interval centered at the point $h_{n=c}$, where $R(h_c)$ has a minimum, or at the center of the interval of stationary $R(h)$. The presence of aerosol in the calibration interval can lead to methodical errors in determination of the components of instrumental vectors. The estimates show that the errors are within the acceptable limits (3–5%), if $R(h) < 1.3$. The algorithm for calculation of $R(h)$ is a modification of the technique from Ref. 5, and it was described by us in Ref. 6. In future studies, we plan to determine $R(h)$ by more accurate technique from Ref. 7, which is based on measurement of Raman signals. The boundaries of the calibration interval are specified by the points h_{c-l} , h_{c+l} , where l are integer numbers of about 10, and, correspondingly, the spatial length of the interval proves to be about 2 km. Particular values depend on the length of the section where C_k are stationary.

In the selected interval, we calculate

$$\bar{C}_k = \frac{1}{2l+1} \sum_{m=-l}^l C_k(h_{c+m}), \quad (7)$$

which are then used to determine the instrumental vectors and the quantum efficiency ratios of the counting channels.

As an illustration of the above-said, Fig. 1*a* depicts all the scattering ratio profiles $R(h)$ obtained in one of the experiments on BSM determination.

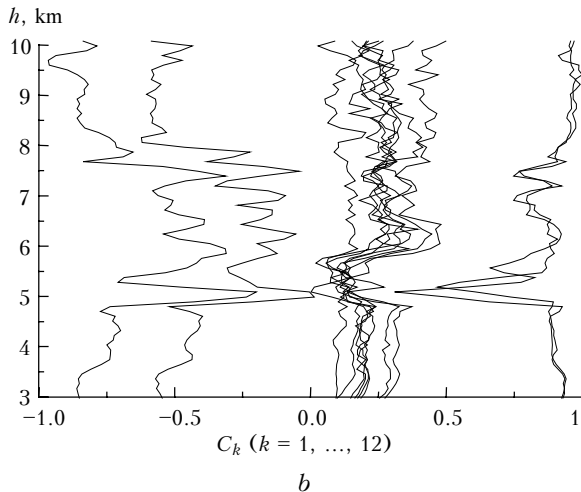
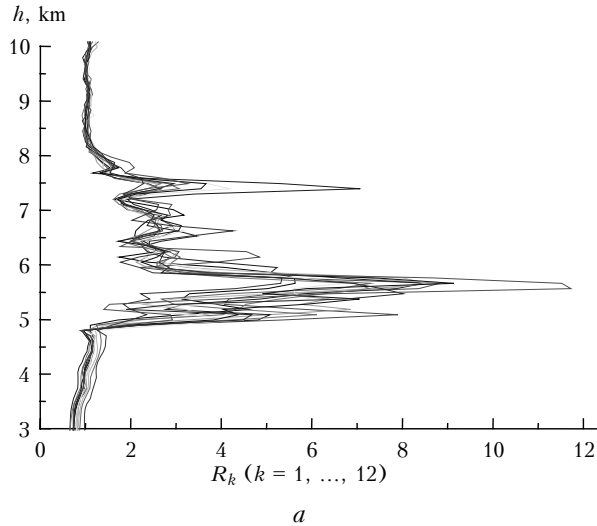


Fig. 1. Altitude profiles of the scattering ratio $R(h)$ (*a*) and altitude profiles of $C_k(h)$ (*b*) obtained on 03.07.2001 in the experiment on measuring backscattering matrices in crystal clouds.

Figure 1 illustrates the multilayer structure of cloudiness and its change from one measurement to another. The interval between the neighboring measurements was, on the average, about 1.5 min. Figure 1*b* depicts the profiles of all twelve C_k obtained in the experiment. One can see that the condition $C_k \cong \text{const}$ and others for the molecular BSM specified above are fulfilled above cloud layers of 8.5 km altitude and higher. The calibration interval in this example occupies the altitudes from 8.5 to 10 km. Application of the algorithm (7) allows us to smooth significant fluctuations arising because of the low level of signals considerably attenuated by clouds. The

accuracy increase at the calibration was noted earlier in Ref. 8.

Determination of the components x_j , y_j , and z_j of the instrumental vectors \mathbf{G}_j and \mathbf{G}_j^* becomes possible at the substitution of \bar{C}_k into the left-hand side of Eq. (5) on the assumption that $\mathbf{M} = \boldsymbol{\sigma}$. After the substitution of Eqs. (3), (4), and (6) into the system (5) and some transformations, it reduces to three (for each j) groups of four equations

$$q_i x_j - u_i y_j - v_i z_j = -[(1 + \alpha_j) \bar{C}_k + \alpha_j - 1] / \sigma [(1 - \alpha_j) \bar{C}_k - \alpha_j - 1], \quad (8)$$

$$i = 1, 2, 3, 4; \quad j = 1, 2, 3; \quad k = 3(i - 1) + j.$$

The equations are determinate, if we know the quantum efficiency ratios of the counting channels α_j . They can be found directly from Eqs. (2). If we substitute Eqs. (3), (4), and (6) into Eq. (2), then we can show that

$$\alpha_j = \sqrt{\bar{N}_{k_1}^{(2)} \bar{N}_{k_2}^{(2)} / (\bar{N}_{k_1}^{(1)} \bar{N}_{k_2}^{(1)})}, \quad (9)$$

$$k_1 = j, \quad k_2 = 3 + j,$$

where the bar above N denotes averaging over the calibration interval similarly to the case of \bar{C}_k [Eq. (7)]. The coefficients α_j can be found by solving two equations (5) simultaneously for \bar{C}_{k_1} and \bar{C}_{k_2} at $\mathbf{M} = \boldsymbol{\sigma}$ and arbitrary values of the components x_j , y_j , z_j of the vectors \mathbf{G}_j . As a result, we have

$$\alpha_j = \sqrt{\frac{(2 - \bar{C}_{k_1} - \bar{C}_{k_2})^2 - (\bar{C}_{k_1} - \bar{C}_{k_2})^2}{(2 + \bar{C}_{k_1} + \bar{C}_{k_2})^2 - (\bar{C}_{k_1} - \bar{C}_{k_2})^2}}. \quad (10)$$

In derivation of Eqs. (9) and (10), we use the different orders of averaging of initial signals, but although the equations look differently, they give the same results.

After the substitution of α_j into equations (8), they can be solved for the components of the instrumental vectors x_j , y_j , z_j . Realization of the above algorithm results in the lidar parameters calibrated against the "molecular reference," which are sufficient for transition to the next step in BSM determination.

2. Calculation of BSM elements for the aerosol component of the atmosphere

With known α_j and the instrumental vectors \mathbf{G}_j , Eqs. (5) can be solved for the elements of \mathbf{M} . This is a matrix of a two-component medium, and it can be represented as a sum of matrices of aerosol \mathbf{A} and molecular $\boldsymbol{\Sigma}$ backscattering:

$$\mathbf{M} = \mathbf{A} + \boldsymbol{\Sigma}.$$

Express \mathbf{M} through the normalized matrices \mathbf{a} and $\boldsymbol{\sigma}$:

$$\mathbf{M} = A_{11} \left[\mathbf{a} + \frac{\Sigma_{11}}{A_{11}} \boldsymbol{\sigma} \right] \quad (11)$$

and note that $\Sigma_{11} = \beta_m$, i.e., it is the molecular backscattering coefficient. This is fulfilled at any state of polarization of the incident radiation \mathbf{S}_i , as follows from the diagonal form of $\boldsymbol{\Sigma}$; $\boldsymbol{\sigma}$ is determined by the equations (6).

The aerosol backscattering coefficient may depend on polarization of the incident radiation. It is the scalar product of the first row of \mathbf{A} (taken as a row vector) and the column vector \mathbf{S}_i , i.e., the Stokes vector of the incident radiation with the unit intensity:

$$\beta_a = A_{11} \mathbf{a}_1 \cdot \mathbf{S}_i, \quad (12)$$

where \mathbf{a}_1 is the row vector formed by the first row of the normalized matrix \mathbf{a} (11).

Combining Eqs. (1), (11), and (12), we can write $\mathbf{M}(h)$ in the following form:

$$\mathbf{M}_k(h) = A_{11,k}(h) \left[\mathbf{a}(h) + \frac{1}{R_k(h) - 1} \mathbf{a}_1(h) \mathbf{S}_i \boldsymbol{\sigma} \right]. \quad (13)$$

The parameters with the index k take different values from one measurement to another because of variability of the aerosol object. Note that at the substitution of Eq. (13) into Eq. (5) the dependence on $A_{11,k}$ disappears, and the object's variability shows itself only through the scattering ratio, which is determined in each of 12 measurements. Since some uncertainty appears in Eq. (13) at $R_k \rightarrow 1$, BSM is calculated for only those altitudes, at which all R_k are not less than 1.25.

Substitution of Eq. (13) into Eq. (5) leads to the vector-matrix equation

$$\begin{aligned} & [C_k(h) - 1] \mathbf{G}_j \mathbf{a}(h) \mathbf{S}_i + \gamma_k(h) \mathbf{a}_1(h) \mathbf{S}_i \mathbf{G}_j \boldsymbol{\sigma} \mathbf{S}_i + \\ & + \alpha_j [C_k(h) + 1] \mathbf{G}_j^* \mathbf{a}(h) \mathbf{S}_i + \gamma_k(h) \mathbf{a}_1(h) \mathbf{S}_i \mathbf{G}_j^* \boldsymbol{\sigma} \mathbf{S}_i = 0, \end{aligned} \quad (14)$$

where

$$\gamma_k(h) = 1/[R_k(h) - 1].$$

This equation is equivalent to the system of 12 linear equations for 16 elements of the normalized BSM of the aerosol component \mathbf{a} . The system becomes determinate and even overdetermined once it is complemented with the normalization condition $a_{11} \equiv 1$ and the BSM symmetry relationships:

$$\begin{aligned} & \text{for } i \neq j \quad a_{ij} = a_{ji}, \text{ if } i \text{ or } j \neq 3, \\ & \text{for } i \neq j \quad a_{ij} = -a_{ji}, \text{ if } i \text{ or } j = 3, \\ & a_{11} - a_{22} - a_{44} + a_{33} = 0. \end{aligned} \quad (15)$$

Here the indices i and j have the meaning different from that all over this paper. The substitution of these relationships into Eq. (14) and simple transformations allow us to write the system of linear equations in the standard vector-matrix form

$$\mathbf{f} = \mathbf{K} \cdot \mathbf{r}. \quad (16)$$

Twelve components of the column vector of free terms are determined by the equation

$$\begin{aligned} f_k = & -(1 + \gamma_k) \frac{(1 + \alpha_j) C_k - 1 + \alpha_j}{(1 - \alpha_j) C_k - 1 - \alpha_j} - \\ & - \sigma \gamma_k (q_i x_j - u_i y_j - v_i z_j) - v_i z_j, \end{aligned} \quad (17)$$

where

$$\begin{aligned} k = & 3(i - 1) + j; \\ f_k = & f_k(h); \quad \gamma_k = \gamma_k(h); \quad C_k = C_k(h). \end{aligned}$$

The column vector of solutions after the substitutions (15) includes eight elements of the normalized BSM of the aerosol component \mathbf{a} :

$$\begin{aligned} r_l = & (a_{12}, a_{13}, a_{14}, a_{22}, a_{23}, a_{24}, a_{33}, a_{34})^T, \\ r_l = & r_l(h); \quad l = 1, 2, \dots, 8. \end{aligned}$$

The first three elements of the k th row of K_{kl} have the form

$$\begin{aligned} K_{k1} = & [x_j - (f_k + v_i z_j) q_i], \quad K_{k2} = -[y_j + (f_k + v_i z_j) u_i], \\ K_{k3} = & [z_j - (f_k + v_i z_j) v_i], \end{aligned}$$

and the others are the linear combinations of the matrix elements

$$\lambda_{ij} = (1 \quad q_i \quad u_i \quad v_i)^T (x_j \quad y_j \quad z_j)$$

of the form $(u_i x_j - q_i y_j)$ and so on.

The excessiveness of the system of equations (16) is used to minimize the errors in determining the elements of \mathbf{a} by the least square method. The algorithm for calculation of the unbiased estimate of \mathbf{r} is expressed by the following equation⁹:

$$\hat{\mathbf{r}} = [\mathbf{K}^T \cdot \mathbf{D}^{-1}(\mathbf{f}) \mathbf{K}]^{-1} \cdot \mathbf{K}^T \cdot \mathbf{D}^{-1}(\mathbf{f}) \mathbf{f}. \quad (18)$$

In the covariance matrix $\mathbf{D}(\mathbf{f})$, only diagonal matrix elements are nonzero, since every component of \mathbf{f} is the result of independent measurement. All arbitrary parameters entering into f_k are functions of the signals $N_k^{(1)}$ and $N_k^{(2)}$. The variance $D(f_k)$ estimated by the rules of error transfer is finally expressed through the estimated variance of signals, whose statistics is assumed to be the Poisson one.

According to Ref. 9, the covariance matrix of estimated errors in the components of \mathbf{r} is determined by the following equation:

$$\mathbf{D}(\mathbf{r}) = \frac{\mathbf{V}^T \cdot \mathbf{D}^{-1}(\mathbf{f}) \mathbf{V}}{n - m} [\mathbf{K}^T \cdot \mathbf{D}^{-1}(\mathbf{f}) \mathbf{K}]^{-1},$$

where $\mathbf{V} = \mathbf{f} - \mathbf{K} \cdot \hat{\mathbf{r}}$ is the residual vector; n and m are ranks of \mathbf{D} and \mathbf{K} .

Calculation of errors allows us to evaluate the reliability of the result obtained and to exclude from consideration BSM, for which the error level exceeds some threshold. The main source of errors is the cloud variability during measurements. This happens

especially often near the cloud boundary, where the scattering ratio and, correspondingly, the parameter γ_k entering into the equation for \mathbf{f} vary widely because of the cloud variability. As an illustration, below we present BSM and the corresponding matrices of the root-mean-square deviations obtained inside a cloud layer and near the cloud boundary:

$$\mathbf{a}(h = 5568 \text{ m}) = \begin{pmatrix} 1 & 0.26 & -0.23 & -0.22 \\ 0.26 & 0.78 & -0.07 & -0.06 \\ 0.23 & 0.07 & -0.56 & -0.09 \\ -0.22 & -0.06 & 0.09 & -0.34 \end{pmatrix},$$

$$\sqrt{D(a_{ij})} = \begin{pmatrix} 0 & 0.03 & 0.01 & 0.01 \\ 0.03 & 0.01 & 0.01 & 0.02 \\ 0.01 & 0.01 & 0.01 & 0.02 \\ 0.01 & 0.02 & 0.02 & 0.02 \end{pmatrix};$$

$$\mathbf{a}(h = 4890 \text{ m}) = \begin{pmatrix} 1 & 0.02 & -0.26 & -0.41 \\ 0.02 & 0.26 & -0.03 & -0.09 \\ 0.26 & 0.03 & -0.32 & -0.07 \\ -0.41 & -0.09 & 0.0 & 0.42 \end{pmatrix},$$

$$\sqrt{D(a_{ij})} = \begin{pmatrix} 0 & 0.07 & 0.04 & 0.08 \\ 0.07 & 0.08 & 0.05 & 0.09 \\ 0.04 & 0.05 & 0.08 & 0.07 \\ 0.08 & 0.09 & 0.07 & 0.12 \end{pmatrix}.$$

This example corresponds to the situation shown in Fig. 1. The first pair of the matrices illustrates the favorable case of measurements, and the second pair corresponds to the doubtful case, which probably will be excluded from a sample for determination of the BSM statistical moments.

Conclusion

Earlier, at the stage of preprocessing of measurements, we have estimated the measurement error in the BSM elements.² For estimation of the r.m.s deviation we used the technique different from that considered in this paper. The estimation was performed with a small sample of BSM corresponding to the centers of cloud layers, where $R(h) \geq 10$. That is, the

selected BSM most probably corresponded to the favorable cases of measurements. The obtained estimate of $\sqrt{D(a_{ij})}$ was ± 0.04 . The advantage of the technique considered is in the fact that it allows the error to be estimated in a single measurement. The tentative analysis of such estimates has shown that the errors in the case of stable cloud layers correspond, generally, to the earlier estimate and often turn to be 2–3 times smaller. This suggests that the considered technique for lidar calibration against the “molecular reference” improves the measurement accuracy, and the calculation algorithm provides for reliable separation of matrices corresponding to the aerosol and molecular atmospheric components.

Acknowledgments

This work was partly supported by the Ministry of Industry, Science and Technologies of Russia (Project “Lidar” No. 06–21) and the Russian Foundation for Basic Research (Grant No. 01–05–65209).

References

1. B.V. Kaul', O.A. Krasnov, A.L. Kuznetsov, and I.V. Samokhvalov, *Atmos. Oceanic Opt.* **4**, No. 4, 303–308 (1991).
2. B.V. Kaul', O.A. Krasnov, A.L. Kuznetsov, E.R. Polovtseva, I.V. Samokhvalov, and A.P. Stykon, *Atmos. Oceanic Opt.* **10**, No. 2, 119–125 (1997).
3. B.V. Kaul' and I.V. Samokhvalov, in: *Regional Monitoring of the Atmosphere. Part 2. New Equipment and Measurement Techniques*, ed. by M.V. Kabanov (Spektr, Tomsk, 1997), pp. 34–58.
4. S.N. Volkov, B.V. Kaul', V.A. Shapranov, and D.I. Shelefontyuk, *Atmos. Oceanic Opt.* **13**, No. 8, 702–706 (2000).
5. R.B. Rassel, J.Y. Swisler, and P.M. McCormick, *Appl. Opt.* **18**, No. 22, 3783–3790 (1979).
6. B.V. Kaul', O.A. Krasnov, and A.L. Kuznetsov, *Izv. Akad. Nauk SSSR, Ser. Fiz. Atmos. Okeana* **24**, No. 8, 824–828 (1988).
7. S.N. Volkov and B.V. Kaul', *Atmos. Oceanic Opt.* **7**, Nos. 11–12, 864–869 (1994).
8. A.P. Chaikovskii, *Atm. Opt.* **3**, No. 11, 1107–1109 (1990).
9. D.J. Hudson, *Statistics. Lectures on Elementary Statistics and Probability* (Geneva, 1964).